PERGAMON

Electrochimica Acta 46 (2001) 2179–2185

ELECTROCHIMICA Acta

www.elsevier.nl/locate/electacta

Structural, optical and electronic properties of $LaMgH_x$ switchable mirrors

J. Isidorsson *, I.A.M.E. Giebels, E.S. Kooij, N.J. Koeman, J.H. Rector, A.T.M. van Gogh, R. Griessen

Faculty of Sciences, Division of Physics and Astronomy, Vrije Universiteit, De Boelelaan 1081, 1081 HV Amsterdam, The Netherlands

Received 29 August 2000; received in revised form 14 November 2000

Abstract

Structural, optical and electronic properties of lanthanum magnesium alloy thin films are studied in situ in real time during hydrogenation. X-ray data show that the as-deposited films contain the intermetallic phase LaMg with CsCl structure as well as fcc β-La and fcc LaH_x. Hydrogenation initiates a transformation of β-La to β-LaH_x, while the intermetallic phase disproportionates. The fcc structure stays intact during further uptake of hydrogen up to LaH_3, and Mg transforms to the rutile structure of MgH_2. During hydrogen absorption the alloys change from a good conducting, metallic state with high reflectance, to a transparent color neutral insulator with a band-gap of about 3 eV.

Keywords: LaMg hydride; Metal–insulator transition; Switchable mirror; X-ray; Optical properties

1. Introduction

Since the remarkable optical properties of yttrium and lanthanum hydride were discovered by Huiberts et al. [1] in 1996, switchable mirrors have received considerable interest. Most work has been devoted to yttrium hydride, but other rare earth metal hydrides have also been investigated [2–5]. From an application point of view it is, however, desirable to have a wider bandgap than that of YH_3. Van der Sluis et al. [2] alloyed gadolinium with magnesium, and reached a color neutral transparent state.

In contrast to yttrium very little has been published on optically switching lanthanum-containing hydrides [6–8]. This is due to the high reactivity of lanthanum. As shown by Van Gogh et al. [9] this difficulty can, however, be overcome by using an AlO_x buffer layer on top of the La film.

In this work we study the structural, electronic and optical properties of LaMg alloys during hydrogenation. The electrical resistivity is measured in situ during the experiments, in order to be able to relate optical and structural measurements with each other.

The purpose of the present investigation is to explore the influence of magnesium on the optical properties of lanthanum hydrides. Although several compositions have been investigated, we focus our attention on a composition close to $La_{0.5}Mg_{0.5}$.

2. Experimental

2.1. Sample preparation

Samples are evaporated on sapphire substrates, or quartz substrates at room temperature or 300°C, in a UHV system with a background pressure of 10^{-9} mbar, using material of typically 99.9% purity. Magne-

* Corresponding author. Fax: +31-20-4447991.

0013-4686/01/$ - see front matter
PII: S0013-4686(01)00373-5

sium is co-evaporated from a Knudsen cell together with lanthanum from an e-beam evaporation source. Two independent crystal quartz microbalances are used to regulate the deposition rates from the two sources. A layer of 1.2 nm aluminum is deposited on top of the lanthanum, and subsequently oxidized to form a protective layer of AlO_x. Finally the film is covered with a 2.5–15-nm thick palladium layer. The role of the palladium is to catalyze the dissociation of H_2 molecules into atomic hydrogen that can be absorbed into the film. Aluminum and palladium are both deposited from a multi-pocket e-beam evaporation unit. For X-ray diffraction we use thick films (typically 500–600 nm) while thin films (typically 50 nm) are used for optical transmittance and reflectance measurements.

2.2. Sample hydrogenation

H_2 loading/unloading is carried out in a vacuum chamber at pressures between 4 and 20 mbar during the loading phase. To reach saturation, i.e. LaH_3 and MgH_2, the pressure is successively increased to 1 bar H_2. Unloading is accomplished by exposing the sample to air and heating it to 50–150°C.

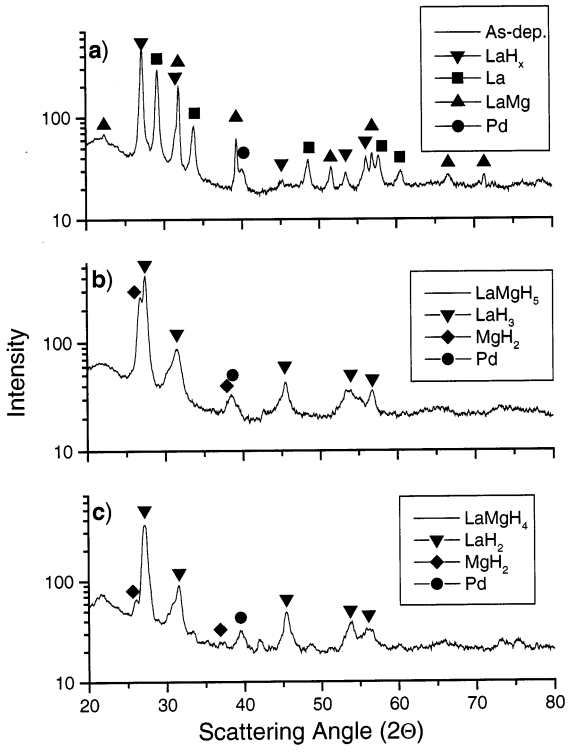

Fig. 1. X-ray spectra of an $LaMgH_x$ film of 584 nm thickness protected by a 10-nm Pd caplayer: (a) as-deposited sample with $x = 0$; (b) sample loaded in room temperature in 1 bar H_2 gas ($x \approx 5$); and (c) after unloading ($x \approx 4$).

2.3. X-ray diffraction

X-ray experiments are performed with Cu K_α radiation in a Rigaku X-ray spectrometer. The samples deposited onto quartz substrates are measured in a θ–2θ configuration, and the samples deposited onto sapphire substrate in a Bragg–Brentano configuration with the incident beam at $\theta = 10°$. The dynamic experiments (during hydrogen loading) are monitored in a relatively limited angular range, usually between 26 and 36° with a scan time of approximately 8 min per spectrum. The hydrogen pressure is chosen so as to result in a total loading time of 5–20 h.

2.4. Optical spectroscopy

Optical measurements are carried out in a Bruker IFS66/S FT-IR spectrometer in the range 354 nm $< \lambda <$ 1722 nm. Transmittance and reflectance at near-normal incidence are recorded continuously during loading/unloading. The loading/unloading pressure is typically 5–20 mbar, and chosen such that during the time it takes for a complete set of reflectance and transmittance spectra to be recorded ($\approx$ 30 s), the sample is essentially in equilibrium with the surrounding H_2 gas. The total loading/unloading time ranged from less than 1 up to 5 h.

2.5. Resistivity

For continuous resistivity measurements the sample is contacted with Al-wires by means of an ultrasonic bonding machine, and connected to a Keithley 2000 Multimeter. Electrical resistivity is measured simultaneously during X-ray scattering experiments, as well as during the recording of the optical spectra. We use Van der Pauw's method [10] to calculate the resistivity.

3. Results and discussion

3.1. X-ray diffraction

Fig. 1 shows the X-ray spectra of a 584-nm thick $La_{0.55}Mg_{0.45}$ film deposited onto a quartz substrate at 300°C. The composition of this sample is determined with the quartz microbalance during deposition. The thickness is confirmed with a DekTac mechanical stylus profilometer. In addition, Rutherford backscattering spectrometry (RBS) is used to control the composition. The composition determined in this way, $La_{0.59}Mg_{0.41}$, is slightly different from that derived from the quartz microbalance during evaporation. This may arise from the fact that in RBS the magnesium signal is difficult to assess because of its overlap with the Si signal of the quartz substrate.

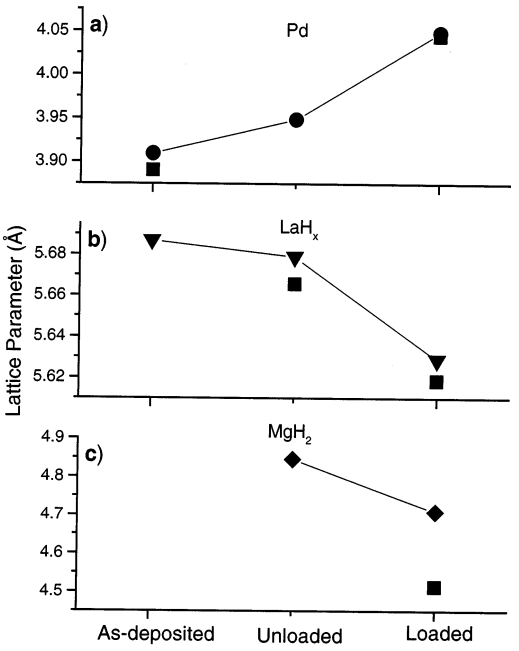

Fig. 2. Lattice parameters for Pd, LaH_x and MgH_2 in a 584-nm thick $La_{0.55}Mg_{0.45}$ film covered with a 10-nm layer of Pd in the as-deposited, unloaded and loaded states. Squares pertain to literature data: (a) Pd; (b) lanthanum hydride; and (c) magnesium.

The spectra are very rich in information, and a number of features can be readily observed. A detailed assignment of the peaks is performed using the program CaRIne and the included database as well as simulations of spectra with data from the literature.

The data for the as-deposited film are shown in Fig. 1a. The simplest material to identify is the LaMg intermetallic compound whose narrow peaks have high intensities. LaMg has a CsCl structure with a small peak at 22.4°, i.e. in a region where the other components have no peaks, and is hence easy to identify. The corresponding lattice spacing of 3.9695 Å is close to the value for bulk LaMg found in literature (3.963 Å) [11].

The bulk low-temperature phase of pure lanthanum has the double hcp (dhcp) structure. In our sample we cannot get a satisfactory fit with the dhcp structure, and we therefore conclude that it is not present. In pure lanthanum thin films deposited at 300°C we notice the same absence of the dhcp structure. This is somewhat surprising, but can be understood as a quenched phase due to the preparation technique used. The transition energy from the low-temperature α-La (dhcp) to the high-temperature β-La (fcc) has an enthalpy of formation of $\Delta H_{\alpha-\beta} = 0.36$ kJ/mol La, which is very small indeed.

Besides β-La we find another fcc structure in the as-deposited sample, i.e. $LaH_{2-\delta}$, where δ is small. Our films have obviously absorbed some hydrogen before the X-ray spectra are recorded. The identification of these two La fcc structures is quite straightforward. The lattice parameter for the high-temperature β-La phase is 5.3045 Å and compares well with the literature value of 5.296 Å [12]. The lattice parameter for lanthanum hydride varies quite substantially during loading/unloading with maximum contraction of 1.02% during loading; this is reported in Fig. 2.

There are no signs of pure magnesium in the samples. This is expected, since, according to the bulk phase diagram, $La_{0.55}Mg_{0.45}$ should contain the intermetallic phase LaMg in a solid solution of lanthanum. Furthermore, if pure magnesium were present, the reflections would be weak and difficult to identify due to the low scattering cross-section of magnesium (40.9) compared to lanthanum (354) [13].

The palladium (111) peak at 39.95° is also easy to identify. The variation of the Pd lattice parameter during loading/unloading is shown in Fig. 2. Palladium expands by 3.6% during loading. Comparing the lattice parameter from our hydrogen loading/unloading experiments with the literature [14] allows us to calculate the hydrogen content in the palladium. In the fully loaded state $H/Pd = 0.67$, which is the saturation level at room temperature and 1 bar H_2 pressure.

The X-ray spectrum of a fully loaded film of approximate composition, $La_{0.55}Mg_{0.45}H_{2.55}$ is more straightforward to analyze than the as-deposited film as there are only three crystallographic structures involved (see Fig. 1b). The intermetallic phase LaMg is disproportionated, and there are no visible peaks left of it. This compares well with the behavior reported for YMg [15]. The $LaH_{3-\delta}$ with fcc structure is fully developed and matches all the major peaks, together with the Pd(111) peak at 38.52°. The MgH_2 rutile lattice, on the other hand, is more subtle to assess as the (200) reflection is situated on the flank of another peak, but the strongest (110) reflection at 26.8° stands out quite clearly. Keeping in mind the low scattering cross-section of magnesium, the assignment of MgH_2 must always be done with great care. In Fig. 2, only the a-axis variation is presented, we notice a contraction of 2.9% during loading. The literature data for MgH_2, $a = 4.517$ Å, $c = 3.021$ Å [16], compare well with our pure MgH_2 data, but are somewhat smaller than $a = 4.71$ Å measured MgH_2 in our hydrogenated LaMg alloy film.

The unloaded "dihydride" film (of approximate composition, $La_{0.55}Mg_{0.45}H_2$) exhibits features that are the same as in the "trihydride" film, see Fig. 1c, except that there are more peaks. Most of the strong peaks can be assigned to LaH_2. The identification of MgH_2 is also reasonably convincing, while the rest of the minor peaks that appeared during the unloading are uncertain.

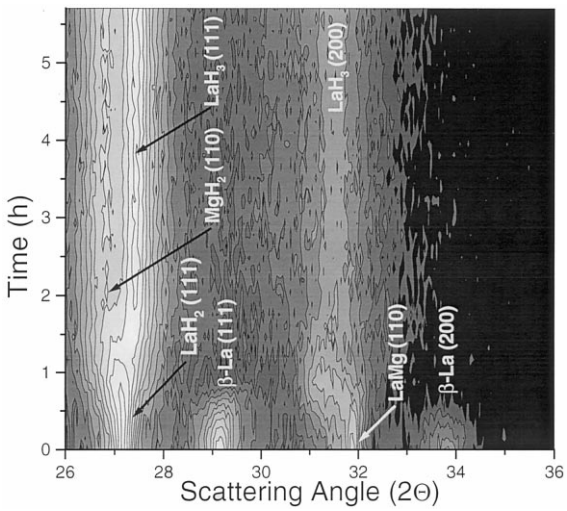

Fig. 3. Structural development of a 584-nm thick $La_{0.55}Mg_{0.45}$ film covered with a 10-nm layer of Pd, recorded with X-ray scattering during hydrogenation at room temperature in 1 bar H_2 gas. Light areas mean high intensity and black low intensity. The β-La disappears after 1 h after which the LaMg phase disproportionates and forms LaH_2 and MgH_2.

The structural development during hydrogenation is followed in situ and in real time. The result of the first loading is presented in Fig. 3. The β-La peaks at 29.2 and 33.8° disappear without any expansion or contraction; this phase clearly does not accommodate hydrogen. By the time the β-La has disappeared, i.e. after 1 h, the LaMg shifts towards lower angle, i.e. expands, before it disappears. The dominant peak at this angle is the LaH_2(200) peak. The major LaH_2(111) peak shifts initially to lower angles in the first phase of loading. This happens while the MgH_2(110) reflection is emerging, and the peak may consequently be the result of two superimposed signals. The LaH_2(111) reappears later in full strength when the MgH_2(110) is fully developed. In this sample the optical metal–insulator transition occurs at around 4 h; this does not involve structural changes as shown in the X-ray scattering spectra.

Table 1
Grain size estimated from the coherence length (in nm) calculated with Eq. (1) for $La_{0.55}Mg_{0.45}$, $La_{0.55}Mg_{0.45}H_{2.55}$ (loaded) and $La_{0.55}Mg_{0.45}H_2$ (unloaded). The indicated major peaks are used for the calculation

Material	As-deposited	Loaded	Unloaded
LaMg(110)	35		
β-La(111)	18		
α-$LaH_{2-\delta}$(111)	21		
γ-$LaH_{3-\delta}$(111)		17	
β-LaH_2(111)			12
MgH_2(110)		13	13
Pd(111)	12	6	6

An estimate of the grain sizes can be obtained from Scherrer's formula,

$$l_{coh} = \frac{0.89\lambda}{\Delta(2\theta)\cos\Theta}, \quad (1)$$

where l_{coh}, the length of coherent scattering, is a measure of the average grain size. In Eq. (1), λ is the wavelength of the X-ray beam (Cu K_α radiation with $\lambda = 1.5418$ Å) and $\Delta(2\theta)$ (in radians) the full width at half maximum (FWHM) of the peak under investigation, Θ is the angle of the peak intensity. The results are presented in Table 1.

The intermetallic LaMg phase has the largest grains with a coherence length of 35 nm. It is interesting to note the reduction of the grain size, particularly the disproportionation of the 35 nm intermetallic LaMg to LaH_x and the decrease in size to 17 and then to 12 nm after the first loading and unloading, respectively. The first decrease in size of the LaH_x phase is of course also associated with the disproportionation of the LaMg phase into LaH_x and MgH_2.

3.2. Optical properties

Optical transmittance and reflectance are also measured in situ in real time during hydrogen loading/unloading. The transmission spectra during a loading experiment of a 50-nm thick $La_{0.51}Mg_{0.49}$ film ($La_{0.54}Mg_{0.46}$ according to RBS), capped with a thin layer of AlO_x and 2.5 nm of palladium is presented in Fig. 4. Four features are of specific interest: (i) a flat plateau in the transmitting state; (ii) the absorption edge close to 400 nm; (iii) the large total transmission change between the unloaded and loaded state; and (iv) the relatively low total transmission in the loaded state.

The first two observations (i, ii) result in an optically color neutral appearance for the human eye. The change by one order of magnitude of the transmission (iii) is achieved with a 50-nm thick active layer, and can easily be tailored within several orders of magnitudes (iv). The transmission in the loaded state is limited by the strong absorption of the 2.5-nm thick palladium layer.

The reflectance spectra are presented in Fig. 5. It is interesting to note the high absorbance, $A = 1 - T - R$, at ≈ 1000 s that happens after the metallic state with high reflectance, but before the transmitting state is reached where the reflectance again increases at certain wavelengths (≈ 800 nm) due to interference. At ≈ 1000 s the condition required for interference is not fulfilled due to absorption and/or scattering in the film.

In Fig. 6 we compare the transmission spectra of LaH_3 and MgH_2 with that of $La_{0.51}Mg_{0.49}H_{2.51}$. The most significant difference is the wider bandgap of the

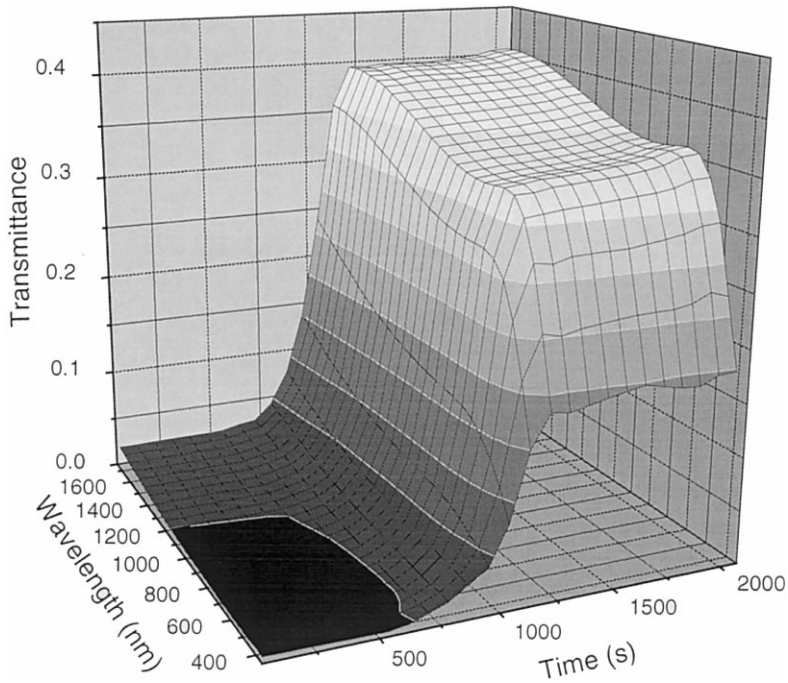

Fig. 4. Evolution of the optical transmittance during hydrogenation of a 50-nm thick $La_{0.51}Mg_{0.49}$ film covered with a 2-nm layer of Pd.

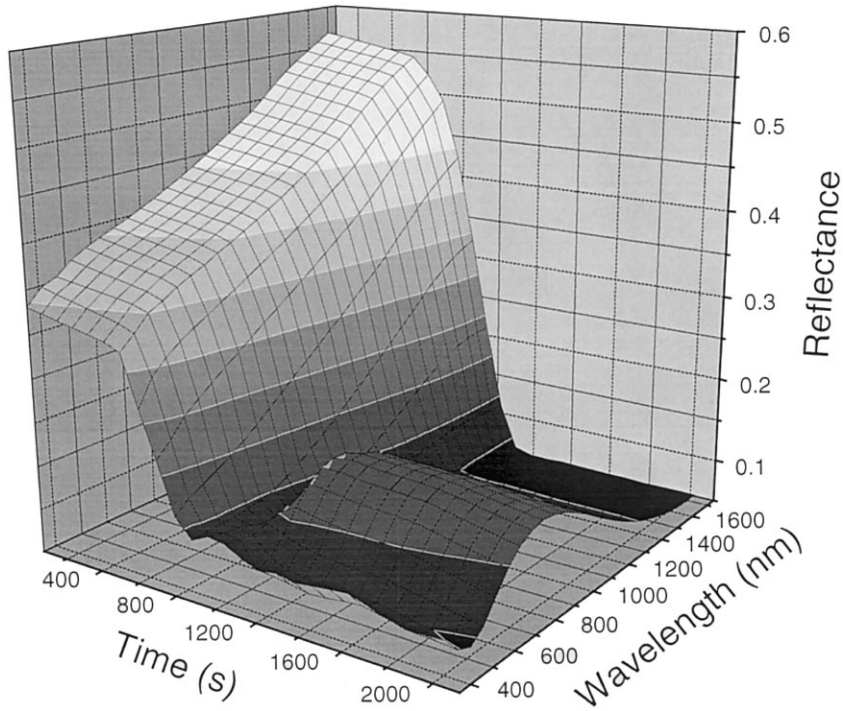

Fig. 5. Evolution of the optical reflectance during hydrogenation of a 50-nm thick $La_{0.51}Mg_{0.49}$ film covered with a 2-nm layer of Pd. The basal plane is rotated 90° compared to Fig. 4 for clarity.

alloy compared to that of pure lanthanum, and hence, the shift of the transmission window towards the UV.

The optical bandgap is estimated by analyzing the transmittance spectra, $T(\omega)$, using the Lambert–Beer law,

$$T(\omega) = T_0 \exp[-\alpha(\omega)d], \quad (2)$$

were α is the absorption coefficient and d the film thickness. The frequency dependence of α near the band edge is related to the optical bandgap E_g through [17]:

$$\alpha(\omega) \propto \frac{(\hbar\omega - E_g)^v}{\hbar\omega}, \quad (3)$$

were v is 2 in disordered materials. Combining these two equations yields,

$$\ln T(\omega) = \ln T_0 - C\frac{(\hbar\omega - E_g)^v}{\hbar\omega}, \quad (4)$$

were C is a constant. The transmission T_0 in the visible is totally dominated by the absorption of the Pd cap layer. It can be considered as constant in the region of the bandgap of LaH_3 and $LaMgH_{2.5}$. From a fit of Eq. (4) to the data in Fig. 6 we find $E_g = 2.2$ eV (563 nm) for the 60-nm thick LaH_3 film, and 3.0 eV (413 nm) for the 50-nm thick $LaMgH_{2.5}$ film The bandgap for the LaH_3 film is higher than that reported by Van Gogh et al. [18] 1.9 eV for a 300-nm thick film. A reason for this difference is that our film is not optically thick. The bandgap of the Mg film is well beyond the limit of the spectrophotometer (3.5 eV), and could not be examined.

The data in Fig. 6 show clearly that the $LaMgH_{2.5}$ film is color neutral and not reddish as compared to the LaH_3 since the part of the optical spectrum visible to the human eye extends from approximately 400 to 700 nm.

3.3. Resistivity

In Fig. 7, the time evolution of the resistivity of a 584-nm thick $LaMgH_x$ alloy is reported together with the optical transmission at $\lambda = 560$ nm and the X-ray intensity at two angles of diffraction pertaining to the β-La(111) and LaH_x(111) peaks. The time-axis for the optical spectra is normalized to that of the X-ray spectra through the in situ resistivity measurements.

There are four regimes of interest: (i) after ≈ 1 h the β-La phase disappears and the electronic resistivity decreases, as LaH_2 is a better conductor than β-La; (ii) during the next phase until ≈ 2 h the intensity of the $LaH_{2-\delta}$-phase saturates, while the resistivity increases only marginally; in region (iii) the reflection of the material decreases as the absorption ($A = 1 - R - T$) increases. The resistivity exhibit local features due to the mixed phases of the conducting $LaH_{2+\delta}$ phase and the insulating $LaH_{3-\delta}$ and MgH_2 phases. Between 3 and 4 h (iv) the $LaH_{3-\delta}$ phase goes through the metal–insulator transition. The resistivity increases drastically and the material becomes transparent.

One should note that in our study we measure the total resistivity of a sample consisting of a 586-nm $LaMgH_x$ alloy covered with a 10-nm PdH_x film. These layers correspond to two resistors in parallel, and hence, the resistivity for the LaMg film and the Pd layer can be calculated with an equivalent parallel circuit. In the as-deposited state the resistivity is very low in both

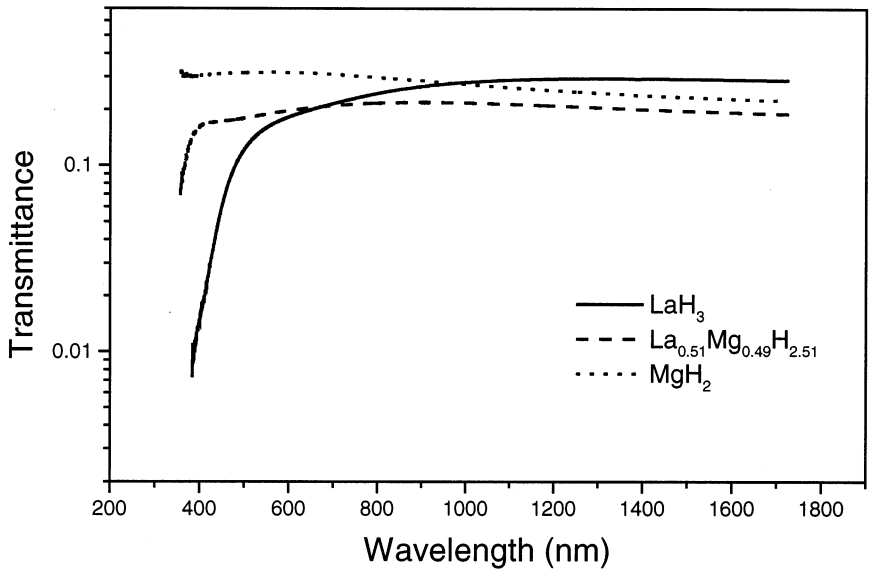

Fig. 6. Transmittance spectra of LaH_3, $La_{0.51}Mg_{0.49}H_{2.51}$ and MgH_2. The LaH_3 film is 60 nm thick, the other two 50 nm.

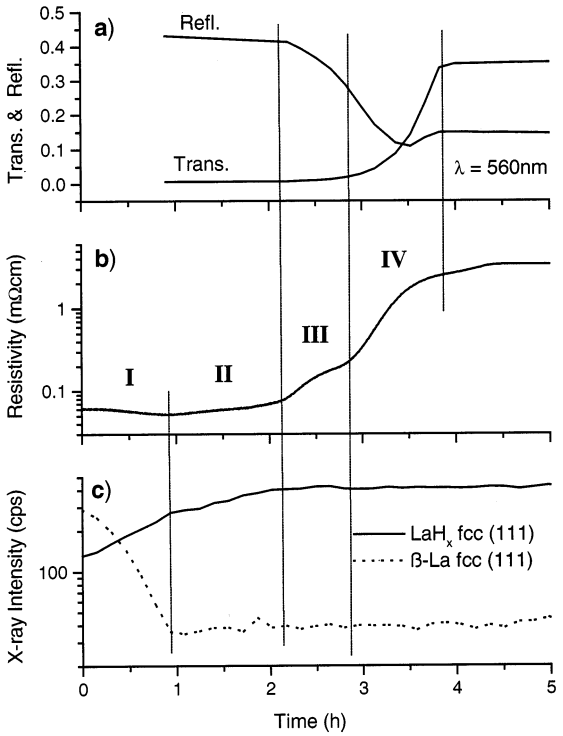

Fig. 7. Time evolution of the transmittance and reflectance at: (a) $\lambda = 560$ nm; (b) resistivity; and (c) X-ray intensity for two dominant peaks in the indicated crystal structures. The indicated regions i–iv in the resistivity spectrum are commented on in the text.

materials, and the influence of Pd is small. However, the difference in resistivity between the fully loaded $PdH_{0.67}$ and $LaMgH_{2.5}$ film is large and the correction is sizeable. For the as-deposited state, the resistivity of PdH_x, as in the as-deposited film, is reported to be 13 μΩ cm [19]. From this we calculate the resistivity of our LaMg film to 66 μΩ cm in the as-deposited state, only slightly higher than the composite resistivity of 61 μΩ cm. The resistivity of pure La is 60–80 μΩ cm for polycrystalline material [13].

4. Conclusions

In this study we have used structural, electronic and optical methods to study $LaMgH_x$. We conclude that $LaMgH_{2.5}$ is an insulator from its high resistivity and its relatively large optical bandgap. The fact that the lanthanum host lattice stays intact during the metal–insulator transition makes lanthanum a prime candidate for studying the influence of hydrogen on the electronic structure of switchable mirror materials. From an application point of view it is interesting to point out that the investigated composition has a color neutral appearance with an optical bandgap of approximately 3 eV.

Acknowledgements

This work is part of the research program of the Stichting voor Fundamenteel Onderzoek der Materie (FOM), financially supported by the Nederlandse Organisatie voor Wetenschappelijk Onderzoek (NWO) and Philips Research, and by the TMR Research Network 'Metal-hydride films with switchable physical properties'.

References

[1] J.N. Huiberts, R. Griessen, J.H. Rector, et al., Nature 380 (1996) 231.
[2] P. van der Sluis, M. Ouwerkerk, P.A. Duine, Appl. Phys. Lett. 70 (1997) 3356.
[3] K. von Rottkay, M. Rubin, P.A. Duine, J. Appl. Phys. 85 (1999) 408.
[4] G.K. Mor, L.K. Malhotra, Thin Solid Films 359 (2000) 28.
[5] D.E. Azofeifa, N. Clark, J. Alloys Compos. 305 (2000) 32.
[6] R. Griessen, J.N. Huiberts, M. Kremers, et al., J. Alloys Compos. 253–254 (1997) 44.
[7] D.J. Peterman, J.H. Weaver, D.T. Peterson, Phys. Rev. B 23 (1981) 3903.
[8] T.J. Udovic, Q. Huang, C. Karmoni, et al., J. Alloys Compos. 293–295 (1999) 113.
[9] A.T.M. van Gogh, S.J. van der Molen, J.W.J. Kerssemakers, et al., Appl. Phys. Lett. 77 (2000) 815.
[10] L.J. Van der Pauw, Philips Res. Rep. 13 (1958) 1.
[11] W.G. Moffat, in: J.H. Westbrook (Ed.), Handbook of binary phase diagrams, Genium Publishing, New York, 1997.
[12] W.B. Pearson, A Handbook of Lattice Spacings and Structures of Metals and Alloys, vol. 2, Pergamon Press, New York, 1967.
[13] R.C. Weast, CRC Handbook of Chemistry and Physics, vol. 59, CRC Press, Boca Raton, FL, 1978.
[14] W.M. Muller, J.P. Blackledge, G.G. Libowitz, Metal Hydrides, Academic Press, New York, 1968.
[15] D.G. Nagengast, A.T.M. van Gogh, E.S. Kooij, et al., Appl. Phys. Lett. 75 (1999) 2050.
[16] R. Yu, P.K. Lam, Phys. Rev. B 37 (1988) 8730.
[17] E.J. Johnson, in: R.K. Willardson, C. Beer (Eds.), Semiconductors and semimetals vol. 3, Academic Press, New York, 1967.
[18] A.T.M. van Gogh, D.G. Nagengast, E.S. Kooij, et al., Phys. Rev. B, to be published.
[19] B.M. Geerken, R. Griessen, J. Phys. F: Met. Phys. 13 (1983) 963.